# Twin Rotor MIMO System Experimental Validation of Robust Adaptive Fuzzy Control Against Wind Effects

Samir Zeghlache , Loutfi Benyettou, Ali Djerioui, and Mohammed Zinelaabidine Ghellab

*Abstract*—In this article, an adaptive fuzzy control (AFC) is synthesized to stabilize the twin rotor multi-input multi-output system (TRMS), to impose then its beam to follow accurately a desired signal or to reach reference positions in 2 DOF. The stability system in the closed-loop has been proved using Lyapunov method, in which all adaptive laws have been generated in order to improve the robustness versus wind gusts, external disturbances, and uncertainties. In addition, the developed control method does not require to decouple the TRMS into main and tail subsystems. Experimental implementation shows the capability of the developed control algorithm.

*Index Terms*—Adaptive control, fuzzy system, robust control, stability, TRMS, wind effects.

## I. INTRODUCTION

RIGID-BODY and flexible systems are real-world control systems problems and are nonlinear in nature. They have disturbances and uncertainties that significantly deteriorate control and tracking, multi-input multi-output and cross coupling effects [1], [2]. For example, helicopters and aircrafts need the use of a robust control algorithm. One of the application domains of the TRMS prototype is to understand flights regimes of these rigid bodies [3]. TRMS illustrates the actual defiance of modern drones control. It is characterized by its capacity to float around a position, high coupling effects, nonlinear and multivariable [4]. For all nonlinear MIMO systems including TRMS, it is very difficult to obtain an efficiency controller. Recently, a several research efforts have been made in the literature to design a robust control of TRMS. For instance, a sliding mode control (SMC) method has been used in [5]–[8] to control TRMS. The SMC is characterized by robustness versus uncertainties and external disturbances. Regrettably, it has a chattering effect which provoke high frequency in the control voltage inputs.

Works mentioned in [6] and [7] proposed solutions in order to reduce the chattering effects but only in simulation, since authors have not elaborated any practical implementation.

Fuzzy logic control has been used extensively to control nonlinear system, where no mathematical models of the controlled systems are known and human experts are obtainable to furnish inference rules. This control technique has been used to control the TRMS system such as in [9] elaborated an interval type-2 fuzzy logic control for TRMS. Neuro-fuzzy and AFC algorithms have been utilized effectively to control nonlinear system such as TRMS. In [10] an adaptive network-based fuzzy inference system and fuzzy subtractive clustering method have been utilized to control the TRMS and to deal with the coupling problems. The main disadvantages of the fuzzy control system is the miss of a systematic methodology for determining the fuzzy control's parameters such as the type of the membership functions and the number of rules. These parameters are frequently adapted manually by trial-and-error technique. Therefore, it is preferable to elaborate an AFC, to ameliorate the performance of the control system based on the adjustment of fuzzy parameters. The fuzzy logic control has been combined with other control methods in order to obtain a good trajectory tracking of the TRMS. For instance, authors in [11] developed a parallel distributed fuzzy linear quadratic control algorithm to the TRMS, to control the vertical and horizontal angles and to obtain a robust trajectory tracking. In [12] a fuzzy logic control has been associated with genetic algorithms and PID control in order to give an optimized control and good robustness versus external disturbances and uncertainties.

Motivated by the precedent problems, this article suggests a robust fuzzy adaptive control to compensate the effects of the uncertainties, external disturbances and coupling effects for TRMS utilizing AFC. This latter has been used in the proposed controller design in order to estimate unknown nonlinear dynamics of the TRMS due to uncertainties. Subsequently, another robust adaptation has been introduced in the proposed control design, in order to reduce the external disturbance effects and to compensate the estimation errors. The system stability in the closed-loop can be assured by the Lyapunov method. In recapitulation, the contributions of this article are as follows.

1) An adaptive fuzzy system has been used in the proposed controller design in order to estimate unknown nonlinear dynamics of the TRMS due to uncertainties and coupling effects. In addition, another adaptive robust control term

has been introduced to reduce the wind gusts, external disturbance effects and to compensate the approximation errors of the adaptive fuzzy system.

2) The system stability in the closed-loop has been proved by utilizing Lyapunov criterion where all adaptive laws have been generated.

3) The developed AFC control has been validated in practical experimentation.

According to the existing works [11], [13]–[25], the contributions of this article can be summarized as follows.

1) The control method proposed to the TRMS in [13] needs a complex nonlinear observer, which will augment the complexity and computational time. In this paper, a robust AFC has been proposed without needing a nonlinear observer.

2) The authors in [14] proposed an adaptive high order sliding mode control for TRMS. This method has proven to be effective to reduce the chattering effect. But it requires the knowledge of the sliding surfaces and its derivatives, and it is very sensitive to noise measurement. Additionally, this control method has been validated only in simulation, without any hardware implementation. However, in this article the developed control strategy has been validated in real time implementation.

3) In [15], multistep feedback linearization control strategy has been proposed for TRMS. The results proved a favorable tracking performance. Unfortunately, this control technique is sensitive to external disturbances. In addition, this control strategy needs a complex nonlinear observer in order to deal with unmeasured states which augment the complexity of the controller which is not desirable in real time implementation. The authors have used the coupled model of TRMS without taking into account the practical experimentation. Whereas, real time implementation has been elaborated to the real TRMS in this article.

4) Differently to [16] and [17] where the stability analysis is not rigorously demonstrated. In this article, the TRMS stability has been clearly proved using Lyapunov criteria, along with TRMS nonlinear coupled model. Moreover, the developed control algorithm does not require decoupling step [16], [11], [18]–[21].

5) The authors in [22] and [23] proposed an hybrid control based on fuzzy sliding mode control for the TRMS, in order to reduce the chattering phenomena. Despite the good results obtained, the practical validation did not take place.

6) The authors in [24] developed a new control strategy based on model predictive control for the TRMS. Another adaptive control method has been proposed in [25], where authors used feedback linearization technique for TRMS. The tracking results of these two types of control algorithms have been validated in experimentation without taking into consideration the wind effects. Contrariwise, in this paper, an AFC algorithm has been designed in order to overcome the wind effects.

According to the cited previous papers, this article adopts an adaptive and robust control approach in the presence of wind
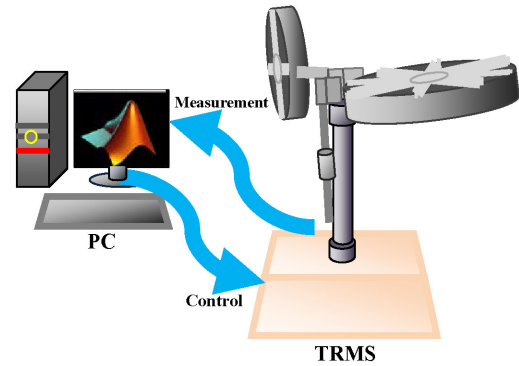


Fig. 1. Configuration of the TRMS.

effects, where the proposed method includes a fuzzy inference system and an adaptive control in order to obtain a best trajectory tracking of TRMS. Afterward, stability analysis has been demonstrated by Lyapunov method. In order to prove capability of the proposed control algorithm, an experimental implementations are performed to the TRMS prototype. The adopted control approach permits to evade the modelling problems, to provide a best robustness and to get a desired trajectory tracking with better precision in attendance of wind effects.

The rest of the article is arranged as follows, in Section II, the TRMS description with dynamic modelling are adopted. Section III presentsthe AFC design, experiment results are provided in Section IV. Finally, conclusions are given in Section V.

## II. TRMS DESCRIPTION

As depicted in Fig. 1, the TRMS is an aero-dynamical system. Its comportment is like helicopter, composed of two perpendicular rotors actuated by dc motors, vertical rotor and horizontal rotor that are put on a beam which contains counter weight. The vertical rotor generates a hoist force permitting the beam to turn in main or vertical plane (pitch angle noted $\psi$), while the horizontal rotor permits the beam to turn in tail or horizontal plane (yaw angle noted $\varphi$). The two rotors are commanded by varying the input voltage of the dc motors. The vertical and horizontal angles are measured by using position sensors placed in the pivot. The TRMS is a multivariable system thatcontains two inputs and two outputs which is characterized by strong coupling and complex dynamics. The system is controlled by utilizing PC (personal computer) and the controller can be implemented in MATLAB/Simulink environment of the interfacing computer to control the real system. The measured and control signals are transmitted by Advantech PCI-1711 card. The physical parameters are shown in Table I.

### A. Dynamics Model of 2-DOF TRMS

The momentum equation for vertical subsystem is given by

$$I_1\ddot{\psi} = M_1 - M_{B\psi} - M_{FG} - M_G \qquad (1)$$

where

TABLE I
PHYSICAL PARAMETERS OF TRMS [27]

| Symbol | Definition | Value |
|---|---|---|
| $I_1$ | Moment of inertia of vertical rotor | $6.8{\times}10^{-2}\ kg.m^2$ |
| $I_2$ | Moment of inertia of horizontal rotor | $2{\times}10^{-2}\ kg.m^2$ |
| $a_1$ | Static characteristic parameter | 0.0135 |
| $b_1$ | Static characteristic parameter | 0.0924 |
| $a_2$ | Static characteristic parameter | 0.02 |
| $b_2$ | Static characteristic parameter | 0.09 |
| $M_g$ | Gravity momentum | 0.32 |
| $B_{1\psi}$ | Friction momentum parameter | $6{\times}10^{-3}\ N.m.s/rad$ |
| $B_{1\varphi}$ | Friction momentum parameter | $1{\times}10^{-1}\ N.m.s/rad$ |
| $K_{gy}$ | Gyroscopic momentum parameter | 0.05 s/rad |
| $K_{gx}$ | Gyroscopic momentum parameter | 0.0163 s/rad |
| $k_{11}$ | Motor 1 gain | 1.1 |
| $k_{22}$ | Motor 2 gain | 0.8 |
| $T_{11}$ | Motor 1 denominator parameter | 1.2 |
| $T_{10}$ | Motor 1 denominator parameter | 1 |
| $T_{22}$ | Motor 2 denominator parameter | 1 |
| $T_{20}$ | Motor 2 denominator parameter | 1 |
| $T_p$ | Cross reaction momentum parameter | 2 |
| $T_0$ | Cross reaction momentum parameter | 3.5 |
| $k_c$ | Cross reaction momentum gain | -0.2 |

$M_1$ is the gross momentum of vertical rotor in relation to generated momentum $\tau_1$ by the first motor, expressed as

$$M_1 = a_1\tau_1^2 + b_1\tau_1. \qquad (2)$$

$M_{B\psi}$ denotes the friction forces momentum written as

$$M_{B\psi} = B_{1\psi}\dot{\psi} - B_{2\psi}\sin(2\psi)\,\dot{\varphi}^2. \qquad (3)$$

$M_{FG}$ presents the gravity momentum described by

$$M_{FG} = M_g\sin(\psi). \qquad (4)$$

$M_G$ denotes the gyroscopic momentum obtained by

$$M_G = K_{gy}M_1\dot{\varphi}\cos(\psi). \qquad (5)$$

In addition, the vertical rotor voltage $u_1$ and produced momentum $\tau_1$ are expressed by a first order transfer function, determined as

$$\tau_1 = \frac{k_{11}}{T_{11}s + T_{10}}u_1. \qquad (6)$$

The momentum equation for horizontal subsystem is given by

$$I_2\ddot{\varphi} = M_2 - M_{B\phi} - M_R \qquad (7)$$

where $M_2$ is the gross momentum of vertical rotor in relation to generated momentum $\tau_2$ by the first motor, expressed as

$$M_2 = a_1\tau_2^2 + b_1\tau_2. \qquad (8)$$

$M_{B\varphi}$ denotes the friction forces momentum written as

$$M_{B\varphi} = B_{1\varphi}\dot{\varphi}. \qquad (9)$$

$M_R$ denotes is the cross reaction momentum expressed by

$$M_R = \frac{k_c(T_0s + 1)}{T_ps + 1}M_1. \qquad (10)$$

$M_R$ can be rewritten in time domain as [26]

$$M_R = 0.375\,k_c e^{-0.5t}M_1 \qquad (11)$$

Finally, the dynamic model is rewritten as

$$\begin{cases} \ddot{\psi} = \frac{1}{I_1}\Big\{-M_g\sin(\psi) - B_{1\psi}\dot{\psi} + k_{gx}\dot{\varphi}^2\sin(2\psi) \\ \quad - \big(a_1\tau_1^2 + b_1\tau_1\big)\big(k_{gy}\dot{\varphi}\cos(\psi) + 1\big) + w_1\Big\} \\ \ddot{\varphi} = \frac{1}{I_2}\Big\{-B_{1\varphi}\dot{\varphi} - \big(0.375\,k_ce^{-0.5t}\big)\big(a_1\tau_1^2 + b_1\tau_1\big) \\ \quad + a_2\tau_2^2 + b_2\tau_2 + w_2\Big\} \end{cases} \qquad (12)$$

where $w_1$ and $w_2$ are the wind effects.

## III. AFC DESIGN

The dynamic model in (12) can be presented in the state-space form as

$$\begin{cases} \dot{x}_1 = x_2 \\ \dot{x}_2 = -\frac{M_g}{I_1}\sin(x_1) - \frac{B_{1\psi}}{I_1}x_2 + \frac{K_{gx}}{I_1}x_4{}^2\sin(2x_1) \\ \quad + \frac{a_1}{I_1}x_5^2 + \frac{b_1}{I_1}x_5\big(1 - K_{gy}x_4\cos(x_1)\big) + w_1 \\ \dot{x}_3 = x_4 \\ \dot{x}_4 = -\frac{B_{1\varphi}}{I_2}x_4 - \frac{M_R}{I_2} + \frac{a_2}{I_2}x_6^2 + \frac{b_2}{I_2}x_6 + w_2 \\ \dot{x}_5 = -\frac{T_{10}}{T_{11}}x_5 + \frac{k_{11}}{T_{11}}u_1 \\ \dot{x}_6 = -\frac{T_{20}}{T_{22}}x_6 + \frac{k_{22}}{T_{22}}u_2 \end{cases} \qquad (13)$$

where the state vector is chosen as

$$x = [x_1, x_2, x_3, x_4, x_5, x_6] = [\psi, \dot{\psi}, \varphi, \dot{\varphi}, \tau_1, \tau_2]^T.$$

The state space model (13) can be reorganized as

$$\begin{cases} \dot{x}_1 = x_2 \\ \dot{x}_2 = f_{v1} + \alpha_1 x_5^2 + \alpha_2 x_5 f_{v2} + w_1 \\ \dot{x}_3 = x_4 \\ \dot{x}_4 = f_{h1} + \alpha_3 x_6^2 + \alpha_4 x_6 + w_2 \\ \dot{x}_5 = \alpha_5 x_5 + \alpha_6 u_1 \\ \dot{x}_6 = \alpha_7 x_6 + \alpha_8 u_2 \end{cases} \qquad (14)$$

where

$$f_{v1} = -\frac{M_g}{I_1}\sin(x_1) - \frac{B_{1\psi}}{I_1}x_2 + \frac{K_{gx}}{I_1}x_4{}^2\sin(2x_1)$$

$$\alpha_1 = \frac{a_1}{I_1}, \quad \alpha_2 = \frac{b_1}{I_1}, \quad f_{v2} = 1 - K_{gy}x_4\cos(x_1)$$

$$f_{h1} = -\frac{B_{1\varphi}}{I_2}x_4 - \frac{M_R}{I_2}\big(a_1\,x_5^2 + b_1\,x_5\big), \quad \alpha_3 = \frac{a_2}{I_2}, \quad \alpha_4 = \frac{b_2}{I_2}$$

$$\alpha_5 = -\frac{T_{10}}{T_{11}}, \quad \alpha_6 = \frac{k_{11}}{T_{11}}, \quad \alpha_7 = -\frac{T_{20}}{T_{22}}, \quad \alpha_8 = \frac{k_{22}}{T_{22}}.$$

The tracking errors variables are defined by

$$e_1 = \psi_d - x_1 \qquad (15)$$

$$e_2 = \varphi_d - x_3. \qquad (16)$$

The filtered tracking errors are defined as

$$s_1 = \left(\lambda_1 + \frac{d}{dt}\right)^{r-1}e_1 \qquad (17)$$

$$s_2 = \left(\lambda_2 + \frac{d}{dt}\right)^{r-1}e_2 \qquad (18)$$

where $r$ is the relative degree of the system, $\lambda_1$ and $\lambda_2$ are positive constants.

The relative degree of the TRMS is $r = 3$. Thus

$$s_1 = \ddot{e}_1 + 2\lambda_1 \dot{e}_1 + \lambda_1^2 e_1 \tag{19}$$

$$s_2 = \ddot{e}_2 + 2\lambda_2 \dot{e}_2 + \lambda_2^2 e_2. \tag{20}$$

The time derivative of (17) and (18) are computed as

$$\dot{s}_1 = \dddot{\psi}_d - F_{v1} - \alpha_5 x_5 F_{v2} - \alpha_6 F_{v2} u_1 - \alpha_2 x_5 F_{v3} - \dot{w}_1 \\ + 2\lambda_1(\ddot{\psi}_d - f_{v1} - \alpha_1 x_5^2 - \alpha_2 x_5 f_{v2} - w_1) + \lambda_1^2(\dot{\psi}_d - x_2) \tag{21}$$

$$\dot{s}_2 = \dddot{\varphi}_d - F_{h1} - \alpha_7 x_6 F_{h2} - \alpha_8 F_{h2} u_2 - \dot{w}_2 \\ + 2\lambda_2(\ddot{\varphi}_d - f_{h1} - \alpha_3 x_6^2 - \alpha_4 x_6 - w_2) + \lambda_2^2(\dot{\varphi}_d - x_4) \tag{22}$$

with

$$F_{v1} = \frac{\partial f_{v1}}{\partial x_1} x_2 + \frac{\partial f_{v1}}{\partial x_2} \dot{x}_2 + \frac{\partial f_{v1}}{\partial x_4} \dot{x}_4$$

$$F_{v2} = 2\alpha_1 x_5 + \alpha_2 f_{v2}$$

$$F_{v3} = \frac{\partial f_{v2}}{\partial x_1} x_2 + \frac{\partial f_{v2}}{\partial x_4} \dot{x}_4$$

$$F_{h1} = \frac{\partial f_{h1}}{\partial x_4} \dot{x}_4 + \frac{\partial f_{h1}}{\partial x_5} \dot{x}_5$$

$$F_{h2} = 2\alpha_3 x_6 + \alpha_4.$$

Define the following Lyapunov function as

$$V = \frac{1}{2} \frac{1}{\alpha_6 F_{v2}} s_1^2 + \frac{1}{2} \frac{1}{\alpha_8 F_{h2}} s_2^2 \tag{23}$$

The time derivative of (23) is computed by

$$\dot{V} = \frac{1}{\alpha_6 F_{v2}} s_1 \dot{s}_1 - \frac{\dot{F}_{v2}}{2\alpha_6 F_{v2}^2} s_1^2 + \frac{1}{\alpha_8 F_{h2}} s_2 \dot{s}_2 - \frac{\dot{F}_{h2}}{2\alpha_8 F_{h2}^2} s_1^2 \tag{24}$$

$$\dot{V} = s_1 \left[ \frac{\dddot{\psi}_d - F_{v1} - \alpha_5 x_5 F_{v2} - \alpha_2 x_5 F_{v3} + \lambda_1^2(\dot{\psi}_d - x_2) - \dot{w}_1}{\alpha_6 F_{v2}} \right. \\ \left. + \frac{2\lambda_1(\ddot{\psi}_d - f_{v1} - \alpha_1 x_5^2 - \alpha_2 x_5 f_{v2} - w_1)}{\alpha_6 F_{v2}} - \frac{\dot{F}_{v2}}{2\alpha_6 F_{v2}^2} s_1 - u_1 \right] \\ + s_2 \left[ \frac{\dddot{\varphi}_d - F_{h1} - \alpha_7 x_6 F_{h2} + \lambda_2^2(\dot{\varphi}_d - x_4) - \dot{w}_2}{\alpha_8 F_{h2}} \right. \\ \left. + \frac{2\lambda_2(\ddot{\varphi}_d - f_{h1} - \alpha_3 x_6^2 - \alpha_4 x_6 - w_2)}{\alpha_8 F_{h2}} - \frac{\dot{F}_{h2}}{2\alpha_8 F_{h2}^2} s_2 - u_2 \right]. \tag{25}$$

The control laws $u_1$ and $u_2$ are given as

$$u_1 = \frac{1}{\alpha_6 F_{v2}} \left[ \dddot{\psi}_d + 2\lambda_1(\ddot{\psi}_d - f_{v1} - \alpha_1 x_5^2 - \alpha_2 x_5 f_{v2} - w_1) \right. \\ \left. - \alpha_5 x_5 F_{v2} - F_{v1} - \alpha_2 x_5 F_{v3} + \lambda_1^2(\dot{\psi}_d - x_2) - \frac{\dot{F}_{v2}}{2F_{v2}} s_1 - \dot{w}_1 \right] \\ + \beta_1 s_1 \tag{26}$$

$$u_2 = \frac{1}{\alpha_8 F_{h2}} \left[ \dddot{\varphi}_d - F_{h1} - \alpha_7 x_6 F_{h2} + \lambda_2^2(\dot{\varphi}_d - x_4) - \frac{\dot{F}_{h2}}{2F_{h2}} s_2 - \dot{w}_2 \right. \\ \left. + 2\lambda_2(\ddot{\varphi}_d - f_{h1} - \alpha_3 x_6^2 - \alpha_4 x_6 - w_2) \right] + \beta_2 s_2 \tag{27}$$

with $\beta_1$ and $\beta_2$ positive constants.

Using (26) and (27), it can be verified that

$$\dot{V} = -\beta_1 s_1^2 - \beta_2 s_2^2 < 0. \tag{28}$$

If we considered a free of wind effects, i.e., $w_1 = \dot{w}_1 = w_2 = \dot{w}_2 = 0$, the ideal control laws are rewritten as

$$u_1 = \frac{1}{\alpha_6 F_{v2}} \left[ \dddot{\psi}_d + 2\lambda_1(\ddot{\psi}_d - f_{v1} - \alpha_1 x_5^2 - \alpha_2 x_5 f_{v2}) - \alpha_5 x_5 F_{v2} \right. \\ \left. - F_{v1} - \alpha_2 x_5 F_{v3} + \lambda_1^2(\dot{\psi}_d - x_2) - \frac{\dot{F}_{v2}}{2F_{v2}} s_1 \right] + \beta_1 s_1 \tag{29}$$

$$u_2 = \frac{1}{\alpha_8 F_{h2}} \left[ \dddot{\varphi}_d - F_{h1} - \alpha_7 x_6 F_{h2} + \lambda_2^2(\dot{\varphi}_d - x_4) - \frac{\dot{F}_{h2}}{2F_{h2}} s_2 \right. \\ \left. + 2\lambda_2(\ddot{\varphi}_d - f_{h1} - \alpha_3 x_6^2 - \alpha_4 x_6) \right] + \beta_2 s_2. \tag{30}$$

The functions $F_{vi}$ $(i = 1, 2, 3)$, $f_{vj}$, $F_{hj}$ $(j = 1, 2)$ and $f_{h1}$ are considered unknown and $w_1, \dot{w}_1, w_2$ and $\dot{w}_2$ expression which include wind effects are different to zero, in this paper an adaptive fuzzy system has been used to overcome this problem. The proposed control strategy concern the online estimation of control laws $u_1$ and $u_2$ given in (26) and (27) by two fuzzy inference systems where the fuzzy parameters are adjusted.

### A. Fuzzy Logic System

The basic structure of a fuzzy logic system consists of a fuzzifier, some fuzzy IF-THEN rules, a fuzzy inference engine and a defuzzifier. The fuzzy IF-THEN rules are written in the following form [28]:

$$R^k: \text{IF } x_1 \text{ is } F_1^k \text{ and } \dots x_n \text{ is, THEN } y_i \text{ is } G^k, k=1, 2, \dots, N \tag{31}$$

where $X = [x_1, \dots, x_n] \in \Re^n$ and $\bar{Y} \in \Re^n$ are the input and the output vectors, respectively. $F_l^k (l = 1, \dots, n)$ and $G^i$ are the fuzzy sets associated with the fuzzy membership functions $\mu_{F_l^k}(x_l)$ and $\mu_{G^k}(\bar{Y})$, respectively. $N$ is the number of rules.

By using the singleton fuzzifier, product inference engine, and center average defuzzification [29], the output of the fuzzy logic system can be given as follows:

$$\bar{Y}(X/W) = \frac{\sum_{k=1}^N \bar{y}_k \prod_{l=1}^n \mu_{F_l^k}(x_l)}{\sum_{k=1}^N \left[ \prod_{l=1}^n \mu_{F_l^k}(x_l) \right]} \tag{32}$$

where $\bar{y}_k = \max_{y \in \Re} \mu_{G^k}(y)$. Let

$$\Theta_i(X) = \frac{\sum_{k=1}^N \prod_{l=1}^n \mu_{F_l^k}(x_l)}{\sum_{k=1}^N \left[ \prod_{l=1}^n \mu_{F_l^k}(x_l) \right]}. \tag{33}$$

Denoting, $\Theta = [\Theta_1(X), \Theta_2(X), \dots, \Theta_N(X)]^T$ as the vector of fuzzy basis functions, and $W^T = [\bar{y}_1, \bar{y}_2, \dots, \bar{y}_N]^T = [W_1, W_2, \dots, W_N]$ the vector of consequent parameters. Then, the fuzzy logic system can be given as

$$\bar{Y}(X/W) = W^T \Theta. \tag{34}$$

In this article, five fuzzy sets {NB: negative big, NS: negative small, ZE: zero environ, PS; positive small, PB: positive big}, are defined for each variable $(e_1, \dot{e}_1)$ and $(e_2, \dot{e}_2)$ as presented in Fig. 2.

The control laws $u_1$ and $u_2$ can be rearranged as [30]

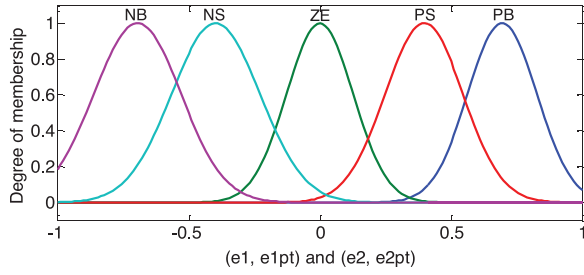$$u_1 = u_{b1} + \beta_1 s_1 \tag{35}$$

Fig. 2.   Fuzzy membership functions.

$$u_2 = u_{b2} + \beta_2 s_2 \tag{36}$$

where

$$u_{b1} = \frac{1}{\alpha_6 F_{v2}} \left[ \ddddot{\psi}_d + 2\lambda_1 \left( \ddot{\psi}_d - f_{v1} - \alpha_1 x_5^2 - \alpha_2 x_5 f_{v2} - w_1 \right) \right. \\ \left. - \alpha_5 x_5 F_{v2} - F_{v1} - \alpha_2 x_5 F_{v3} + \lambda_1^2 (\dot{\psi}_d - x_2) - \frac{\dot{F}_{v2}}{2 F_{v2}} s_1 - \dot{w}_1 \right] \tag{37}$$

$$u_{b1} = \frac{1}{\alpha_8 F_{h2}} \left[ \ddddot{\varphi}_d - F_{h1} - \alpha_7 x_6 F_{h2} + \lambda_2^2 (\dot{\varphi}_d - x_4) - \frac{\dot{F}_{h2}}{2 F_{h2}} s_2 \right. \\ \left. - \dot{w}_2 + 2\lambda_2 \left( \ddot{\varphi}_d - f_{h1} - \alpha_3 x_6^2 - \alpha_4 x_6 - w_2 \right) \right]. \tag{38}$$

The control laws $u_{b1}$ and $u_{b2}$ can be estimated by a fuzzy inference system as

$$\hat{u}_{b1} = W_1^T (e_1, \dot{e}_1) \, \Theta_1 \tag{39}$$

$$\hat{u}_{b2} = W_2^T (e_2, \dot{e}_2) \, \Theta_2 \tag{40}$$

where $\Theta_1$ and $\Theta_2$ represent adapted vector parameters, and $W_1^T(e_1, \dot{e}_1)$ and $W_2^T(e_2, \dot{e}_2)$ denote basis functions given a fuzzy inference system.

The real control law $u_{b1}$ and $u_{b2}$ is expressed by

$$u_{b1} = W_1^T (e_1, \dot{e}_1) \, \Theta_1^* + \varepsilon_1 \tag{41}$$

$$u_{b2} = W_2^T (e_2, \dot{e}_2) \, \Theta_2^* + \varepsilon_2 \tag{42}$$

where $\Theta_1^*$ and $\Theta_2^*$ are the optimal parameters, and $\varepsilon_1$ and $\varepsilon_2$ are the estimation error that satisfy the following condition:

$$\begin{cases} |\varepsilon_1| \leq \bar{\varepsilon}_1 \\ |\varepsilon_2| \leq \bar{\varepsilon}_2 \end{cases} \tag{43}$$

where $\bar{\varepsilon}_1$ and $\bar{\varepsilon}_2$ are unknown positive parameters.

The adaptive control laws applied to the TRMS are written by [30]

$$u_1 = u_{a_1} + u_{r_1} + u_{p_1} \tag{44}$$

$$u_2 = u_{a_2} + u_{r_2} + u_{p_2} \tag{45}$$

with

1) $u_{a_1}$ and $u_{a_2}$ are the fuzzy adaptive control expression which is synthesized in order to estimate the ideal control laws $u_{b1}$ and $u_{b2}$ given as

$$u_{a_1} = \hat{u}_{b1} = W_1^T (e_1, \dot{e}_1) \, \Theta_1 \tag{46}$$

$$u_{a_2} = \hat{u}_{b2} = W_2^T (e_2, \dot{e}_2) \, \Theta_2 \tag{47}$$

and $\Theta_1$ and $\Theta_2$ are the adapted vector parameters expressed as

$$\dot{\Theta}_1 = \gamma_1 s_1 W_1^T (e_1, \dot{e}_1) - \sigma_1 \Theta_1 \tag{48}$$

$$\dot{\Theta}_2 = \gamma_2 s_2 W_2^T (e_2, \dot{e}_2) - \sigma_2 \Theta_2 \tag{49}$$

where $\gamma_1, \gamma_2, \sigma_1,$ and $\sigma_2$ are designed positive constants, and $\Theta_1(0) = 0, \Theta_2(0) = 0$.

2) $u_{r_1}$ and $u_{r_2}$ are a robust control term are introduced in order to reduce both the effects of fuzzy estimation error and wind effects determined in [31] as

$$u_{r_1} = \hat{\varepsilon}_1 \tanh \left( \frac{s_1}{\chi_1} \right) \tag{50}$$

$$u_{r_2} = \hat{\varepsilon}_2 \tanh \left( \frac{s_2}{\chi_2} \right) \tag{51}$$

where

$$\dot{\hat{\varepsilon}}_1 = \eta_1 s_1 \tanh \left( \frac{s_1}{\chi_1} \right) - \sigma_3 \hat{\varepsilon}_1 \tag{52}$$

$$\dot{\hat{\varepsilon}}_2 = \eta_2 s_2 \tanh \left( \frac{s_2}{\chi_2} \right) - \sigma_4 \hat{\varepsilon}_2 \tag{53}$$

with $\eta_1, \eta_2, \sigma_3, \sigma_4, \chi_1$ and $\chi_2$ are designed positive constants, and $\hat{\varepsilon}_1(0) = 0, \hat{\varepsilon}_2(0) = 0$.

3) $u_{p_1}$ and $u_{p_2}$ are obtained as

$$u_{p_1} = \beta_1 s_1 \tag{54}$$

$$u_{p_2} = \beta_2 s_2 \tag{55}$$

where $\beta_1$ and $\beta_2$ are designed positive constants.

### B. Stability Analysis

Let us define the following Lyapunov functions as

$$V = \frac{1}{2} \frac{1}{\alpha_6 F_{v2}} s_1^2 + \frac{1}{2} \frac{1}{\alpha_8 F_{h2}} s_2^2 + \frac{1}{2\gamma_1} \tilde{\Theta}_1^T \tilde{\Theta}_1 \\ + \frac{1}{2\gamma_2} \tilde{\Theta}_2^T \tilde{\Theta}_2 + \frac{1}{2\eta_1} \tilde{\varepsilon}_1^T \tilde{\varepsilon}_1 + \frac{1}{2\eta_2} \tilde{\varepsilon}_2^T \tilde{\varepsilon}_2. \tag{56}$$

$\tilde{\Theta}_1, \tilde{\Theta}_2, \tilde{\varepsilon}_1,$ and $\tilde{\varepsilon}_2$ are the estimation errors defined by

$$\tilde{\Theta}_1 = \Theta_1^* - \Theta_1 \tag{57}$$

$$\tilde{\Theta}_2 = \Theta_2^* - \Theta_2 \tag{58}$$

$$\tilde{\varepsilon}_1 = \varepsilon_1^* - \hat{\varepsilon}_1 \tag{59}$$

$$\tilde{\varepsilon}_2 = \varepsilon_2^* - \hat{\varepsilon}_2. \tag{60}$$

The time derivative of (56) is computed as

$$\dot{V} = s_1 (u_{b1} - u_1) + s_2 (u_{b2} - u_2) + \frac{1}{\gamma_1} \tilde{\Theta}_1^T \dot{\tilde{\Theta}}_1 + \frac{1}{\eta_1} \tilde{\varepsilon}_1^T \dot{\tilde{\varepsilon}}_1 \\ + \frac{1}{\gamma_2} \tilde{\Theta}_2^T \dot{\tilde{\Theta}}_2 + \frac{1}{\eta_2} \tilde{\varepsilon}_2^T \dot{\tilde{\varepsilon}}_2. \tag{61}$$

By replacing (41), (42), (44), (45), (46), (47), (54), and (55) in (61), we get

$$
\begin{aligned}
\dot{V} \leq\; & s_1\big(W_1^T\,(e_1,\dot{e}_1)\,\Theta_1^* + \varepsilon_1 - W_1^T\,(e_1,\dot{e}_1)\,\Theta_1 - u_{r_1} - \beta_1 s_1\big) \\
& + \tfrac{1}{\gamma_1}\tilde{\Theta}_1^T\dot{\Theta}_1 + \tfrac{1}{\eta_1}\tilde{\varepsilon}_1^T\dot{\varepsilon}_1 + \tfrac{1}{\gamma_2}\tilde{\Theta}_2^T\dot{\Theta}_2 + \tfrac{1}{\eta_2}\tilde{\varepsilon}_2^T\dot{\varepsilon}_2 \\
& + s_2\big(W_2^T(e_2,\dot{e}_2)\Theta_2^* + \varepsilon_2 - W_2^T(e_2,\dot{e}_2)\Theta_2 - u_{r_2} - \beta_2 s_2\big).
\end{aligned}
\tag{62}
$$

Note that the ideal parameter vector $\Theta_1^*$ and $\Theta_2^*$ are an artificial constant quantity introduced only for analysis purpose and its value is not needed when implementing the controller. However, we need the following assumption for the ideal parameter vector [29], [32].

*Assumption* [32]: The ideal parameter vector satisfies

$$
\|\Theta_1^*\| \leq M_{\Theta_1} \text{ and } \|\Theta_2^*\| \leq M_{\Theta_2}
\tag{63}
$$

where $M_{\Theta_1}$ and $M_{\Theta_2}$ are unknown positive constants.

$$
\dot{\tilde{\Theta}}_1 = -\dot{\Theta}_1
\tag{64}
$$

$$
\dot{\tilde{\Theta}}_2 = -\dot{\Theta}_2
\tag{65}
$$

$$
\dot{\tilde{\varepsilon}}_1 = -\dot{\hat{\varepsilon}}_1
\tag{66}
$$

$$
\dot{\tilde{\varepsilon}}_2 = -\dot{\hat{\varepsilon}}_2
\tag{67}
$$

Substituting (64), (65), (66), and (67) into (62) and taking account (57), (58), (59), and (60) we obtain

$$
\begin{aligned}
\dot{V} \leq\; & -\beta_1 s_1^2 - \beta_2 s_2^2 + s_1 W_1^T\,(e_1,\dot{e}_1)\,\tilde{\Theta}_1 + s_2 W_2^T\,(e_2,\dot{e}_2)\,\tilde{\Theta}_2 \\
& + s_1\,(\varepsilon_1 - u_{r_1}) + s_2\,(\varepsilon_2 - u_{r_2}) - \tfrac{1}{\gamma_1}\tilde{\Theta}\dot{\Theta}_1 - \tfrac{1}{\eta_1}\tilde{\varepsilon}_1^T\dot{\hat{\varepsilon}}_1 \\
& - \tfrac{1}{\gamma_2}\tilde{\Theta}_2^T\dot{\Theta}_2 - \tfrac{1}{\eta_2}\tilde{\varepsilon}_2^T\dot{\hat{\varepsilon}}_2.
\end{aligned}
\tag{68}
$$

By introducing (48), (49), (52), and (53) into (68), we get

$$
\begin{aligned}
\dot{V} \leq\; & -\beta_1 s_1^2 - \beta_2 s_2^2 + s_1\,(\varepsilon_1 - u_{r_1}) + s_2\,(\varepsilon_2 - u_{r_2}) + \tfrac{\sigma_1}{\gamma_1}\tilde{\Theta}_1^T\Theta_1 \\
& - \tfrac{1}{\eta_1}\tilde{\varepsilon}_1\eta_1 s_1\,\tanh\!\left(\tfrac{s_1}{\chi_1}\right) + \tfrac{\sigma_3}{\eta_1}\tilde{\varepsilon}_1\hat{\varepsilon}_1 + \tfrac{\sigma_2}{\gamma_2}\tilde{\Theta}_2^T\Theta_2 \\
& - \tfrac{1}{\eta_2}\tilde{\varepsilon}_2\eta_2 s_2\,\tanh\!\left(\tfrac{s_2}{\chi_2}\right) + \tfrac{\sigma_4}{\eta_2}\tilde{\varepsilon}_2\hat{\varepsilon}_2.
\end{aligned}
\tag{69}
$$

Substituting (59) and (60) into (69) we obtain

$$
\begin{aligned}
\dot{V} \leq\; & -\beta_1 s_1^2 - \beta_2 s_2^2 + s_1\,(\varepsilon_1 - u_{r_1}) + s_2\,(\varepsilon_2 - u_{r_2}) + \tfrac{\sigma_1}{\gamma_1}\tilde{\Theta}_1^T\Theta_1 \\
& - \varepsilon_1^* s_1 \tanh\!\left(\tfrac{s_1}{\chi_1}\right) + \hat{\varepsilon}_1 s_1 \tanh\!\left(\tfrac{s_1}{\chi_1}\right) + \tfrac{\sigma_3}{\eta_1}\tilde{\varepsilon}_1\hat{\varepsilon}_1 + \tfrac{\sigma_2}{\gamma_2}\tilde{\Theta}_2^T\Theta_2 \\
& - \varepsilon_2^* s_2 \tanh\!\left(\tfrac{s_2}{\chi_2}\right) + \hat{\varepsilon}_2 s_2 \tanh\!\left(\tfrac{s_2}{\chi_2}\right) + \tfrac{\sigma_4}{\eta_2}\tilde{\varepsilon}_2\,\hat{\varepsilon}_2
\end{aligned}
\tag{70}
$$

or equivalently

$$
\begin{aligned}
\dot{V} \leq\; & -\beta_1 s_1^2 - \beta_2 s_2^2 + \tfrac{\sigma_1}{\gamma_1}\tilde{\Theta}_1^T\Theta_1 - \varepsilon_1^* s_1 \tanh\!\left(\tfrac{s_1}{\chi_1}\right) \\
& + \hat{\varepsilon}_1 s_1 \tanh\!\left(\tfrac{s_1}{\chi_1}\right) + \tfrac{\sigma_3}{\eta_1}\tilde{\varepsilon}_1\hat{\varepsilon}_1 - s_1 u_{r_1} + |s_1|\varepsilon_1^* + \tfrac{\sigma_2}{\gamma_2}\tilde{\Theta}_2^T\Theta_2
\end{aligned}
$$

$$
\begin{aligned}
& -\varepsilon_2^* s_2\,\tanh\!\left(\tfrac{s_2}{\chi_2}\right) + \hat{\varepsilon}_2 s_2\,\tanh\!\left(\tfrac{s_2}{\chi_2}\right) + \tfrac{\sigma_4}{\eta_2}\tilde{\varepsilon}_2\hat{\varepsilon}_2 \\
& - s_2 u_{r_2} + |s_2|\,\varepsilon_2^*.
\end{aligned}
\tag{71}
$$

By introducing (50) and (51) into (71), we get

$$
\begin{aligned}
\dot{V} \leq\; & -\beta_1 s_1^2 - \beta_2 s_2^2 + \tfrac{\sigma_1}{\gamma_1}\tilde{\Theta}_1^T\Theta_1 + |s_1|\,\varepsilon_1^* - \varepsilon_1^* s_1\,\tanh\!\left(\tfrac{s_1}{\chi_1}\right) \\
& + \tfrac{\sigma_3}{\eta_1}\tilde{\varepsilon}_1\hat{\varepsilon}_1 + \tfrac{\sigma_2}{\gamma_2}\tilde{\Theta}_2^T\Theta_2 + |s_2|\,\varepsilon_2^* - \varepsilon_2^* s_2\,\tanh\!\left(\tfrac{s_2}{\chi_2}\right) \\
& + \tfrac{\sigma_4}{\eta_2}\tilde{\varepsilon}_2\hat{\varepsilon}_2.
\end{aligned}
\tag{72}
$$

Consider the inequality written as follows for any value of $\zeta > 0$ [26]:

$$
|s| - s\,\tanh\!\left(\tfrac{s}{\chi}\right) \leq \zeta\chi = \varsigma
\tag{73}
$$

where $\zeta$ is a constant that verifies $\zeta = e^{-(\zeta+1)}$, i.e., $\zeta = 0.2785$.

Equation (72) can be changed as follows:

$$
\begin{aligned}
\dot{V} \leq\; & -\beta_1 s_1^2 - \beta_2 s_2^2 + \varepsilon_1^* \varsigma_1 + \tfrac{\sigma_1}{\gamma_1}\tilde{\Theta}_1^T\Theta_1 + \tfrac{\sigma_3}{\eta_1}\tilde{\varepsilon}_1\hat{\varepsilon}_1 + \varepsilon_2^*\varsigma_2 \\
& + \tfrac{\sigma_2}{\gamma_2}\tilde{\Theta}_2^T\Theta_2 + \tfrac{\sigma_4}{\eta_2}\tilde{\varepsilon}_2\hat{\varepsilon}_2.
\end{aligned}
\tag{74}
$$

By utilizing Young's inequality, one has

$$
\tfrac{\sigma_j}{\gamma_j}\tilde{\Theta}_j^T\Theta_j \leq -\tfrac{\sigma_j}{2\gamma_j}\tilde{\Theta}_j^T\tilde{\Theta}_j + \tfrac{\sigma_j}{2\gamma_j}\tilde{\Theta}_j^{*T}\Theta_j^* \quad j = 1, 2
\tag{75}
$$

$$
\tfrac{\sigma_l}{\eta_j}\tilde{\varepsilon}_j^T\hat{\varepsilon}_j \leq -\tfrac{\sigma_2}{2\eta_j}\tilde{\varepsilon}_j^2 + \tfrac{\sigma_2}{2\eta_j}\left|\varepsilon_j^*\right|^2 \quad j = 1, 2 \text{ and } l = 3, 4.
\tag{76}
$$

By introducing (75) and (76) into (74), we get

$$
\begin{aligned}
\dot{V} \leq\; & -\beta_1 s_1^2 - \beta_2 s_2^2 + \varepsilon_1^*\varsigma_1 - \tfrac{\sigma_1}{2\gamma_1}\tilde{\Theta}_1^T\Theta_1 + \tfrac{\sigma_1}{2\gamma_1}\tilde{\Theta}_1^{*T}\Theta_1^* - \tfrac{\sigma_3}{2\eta_1}\tilde{\varepsilon}_1^2 \\
& + \tfrac{\sigma_3}{2\eta_1}|\varepsilon_1^*|^2 + \varepsilon_2^*\varsigma_2 - \tfrac{\sigma_2}{2\gamma_2}\tilde{\Theta}_2^T\Theta_2 + \tfrac{\sigma_2}{2\gamma_2}\tilde{\Theta}_2^{*T}\Theta_2^* \\
& - \tfrac{\sigma_4}{2\eta_2}\tilde{\varepsilon}_2^2 + \tfrac{\sigma_4}{2\eta_2}|\varepsilon_2^*|^2.
\end{aligned}
\tag{77}
$$

Let us specify

$$
c = \min\{\sigma_1, \sigma_2, \sigma_3, \sigma_4, 2\beta_1\,\alpha_6 F_{v2}, 2\beta_2\,\alpha_8 F_{h2}\}.
\tag{78}
$$

Equation (77) becomes

$$
\dot{V} \leq -cV + \rho
\tag{79}
$$

with

$$
\begin{aligned}
\rho =\; & \varepsilon_1^*\varsigma_1 + \tfrac{\sigma_1}{2\gamma_1}\tilde{\Theta}_1^{*T}\Theta_1^* + \tfrac{\sigma_3}{2\eta_1}|\varepsilon_1^*|^2 \\
& + \varepsilon_2^*\varsigma_2 + \tfrac{\sigma_2}{2\gamma_2}\tilde{\Theta}_2^{*T}\Theta_2^* + \tfrac{\sigma_4}{2\eta_2}|\varepsilon_2^*|^2.
\end{aligned}
\tag{80}
$$

By integrating (77), we get

$$
V(t) \leq V(0)\,e^{-ct} + \tfrac{\rho}{c}.
\tag{81}
$$

From (77) it can be proved that the proposed control laws of TRMS depicted in (44) and (45) are stable despite the existence

This article has been accepted for inclusion in a future issue of this journal. Content is final as presented, with the exception of pagination.

ZEGHLACHE *et al.*: TWIN ROTOR MIMO SYSTEM EXPERIMENTAL VALIDATION OF ROBUST ADAPTIVE FUZZY CONTROL 7
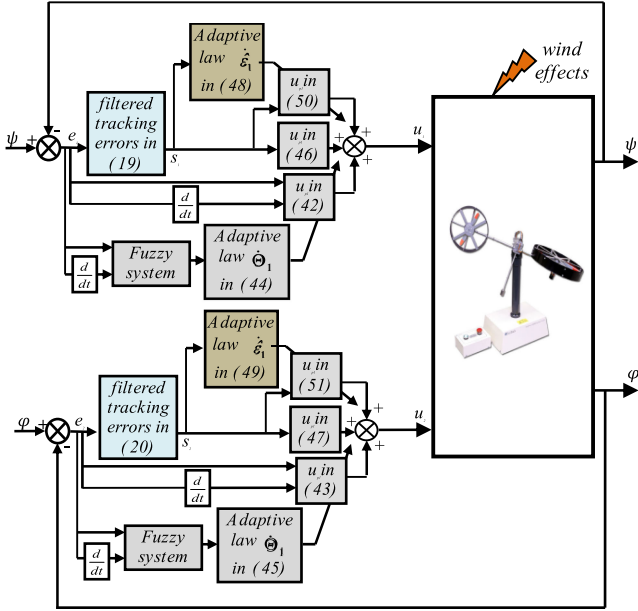


Fig. 3.  Proposed fuzzy adaptive control strategy.

TABLE II
COMPARISON BETWEEN THE CONTROL SCHEME OF THIS
ARTICLE AND [33]–[35]

| Papers [33-35] | This paper |
|---|---|
| - Non adaptive robust control term has been introduced | - An adaptive robust control term has been introduced to reduce the wind gusts, external disturbance effects, and to compensate the approximation errors of the adaptive fuzzy system. |
| - Validated only in simulation. | |
| | - validated in practical experimentation. |

of wind effects consequently the tracking errors converge to zero.

The developed control strategy is presented in Fig. 3.

*Remark:* To highlight the theoretical contributions of this article, a comparative study between this article and [33]–[34] is given in Table II.

## IV. EXPERIMENT RESULTS

The composition of the experimental workbench is presented in Fig. 5, is composed by 33-220 TRMS unit, PC, Advantech PCI 1711 card, feedback cable adaptor box, and an on/off switch box. The voltages control signals are transmitted to the TRMS, which lead the rotors. The measures of vertical and horizontal angle of the beam ($\psi$ and $\varphi$ angles) are obtained by utilizing digital encoders sensor. The measured angles are transmitted to the PC by using the interface unit. In this article, a PC (Intel Core 3.00 GHz processor, 1 GB RAM) with 32-bit XP-Windows operating

system and MATLAB/Simulink environment are utilized in order to implement the proposed control algorithm. The complete MATLAB/Simulink block diagram is presented in Fig. 4.

The proposed controller was implemented using MATLAB/Simulink, a graphical programming language tool developed by MathWorks. The control design flow diagram is depicted in Fig. 5. The Simulink model is transferred to real-time workshop (RTW) to build a C++ source program. C++ compiler compiles and links this program to produce an executable code. Real-Time Windows target is used as an interface between the created executable program acting as the control program and the input/output (I/O) board [27].

The developed control strategy has demonstrated to be effective as regards to several desired signal which encompass diverse operating regions. The tracking responses of the TRMS in experiment are depicted in Figs. 6–11.

### A. Test1: Sine Wave Tracking

The experiment results presented in Figs. 6 and 7 clarify the tracking responses of the TRMS according to sine desired signals for vertical and horizontal angles. The evolutions in experimental results of vertical angle ($\psi$) and horizontal angle ($\varphi$) illustrated in Fig. 6(a) and (b), prove the capability of the developed control algorithm in the trajectory pursuit problem. In addition, Fig. 7 presents the performed trajectory of the TRMS, as regards to sine desired trajectory with different frequencies in experiment, to prove the effectiveness of the developed control strategy to overcome with coupling effects between the two subsystems. The control input signals depicted in experimental results [Fig. 6(c) and (d)] for vertical and horizontal dc motors, shows their limitations in the admitted interval.

### B. Test2: Triangle Wave Tracking

The effectiveness of the developed control algorithm in experimentation with triangle desired trajectories are shown in Figs. 8 and 9. The performances of the controlled TRMS in trajectory tracking is confirmed in these figures. It is observed that tracking effectiveness are proved in practical implementation as shown in Fig. 8(a) and (b).

Fig. 9(a) and (b) illustrates the performed trajectories of the TRMS with respect to triangle reference trajectory with different frequencies in experiment implementation. It is clear that the proposed control algorithm can handle the coupling effects between the horizontal and vertical subsystems, after low overshoot in the experimental responses of pitch and yaw angles as shown in Fig. 9(a) and (b) due to the nature of the triangle signals. The main and tail control input voltages depicted in experimental results [Fig. 8(c) and (d) and Fig. 9(c) and (d)] are bounded in the permit interval.

### C. Test3: Square Wave Tracking

To process the regulation task of the TRMS, square desired trajectories for vertical and horizontal angles are considered. The experimental results are presented in Figs. 10 and 11. It is obvious that the developed control strategy is able to treat the
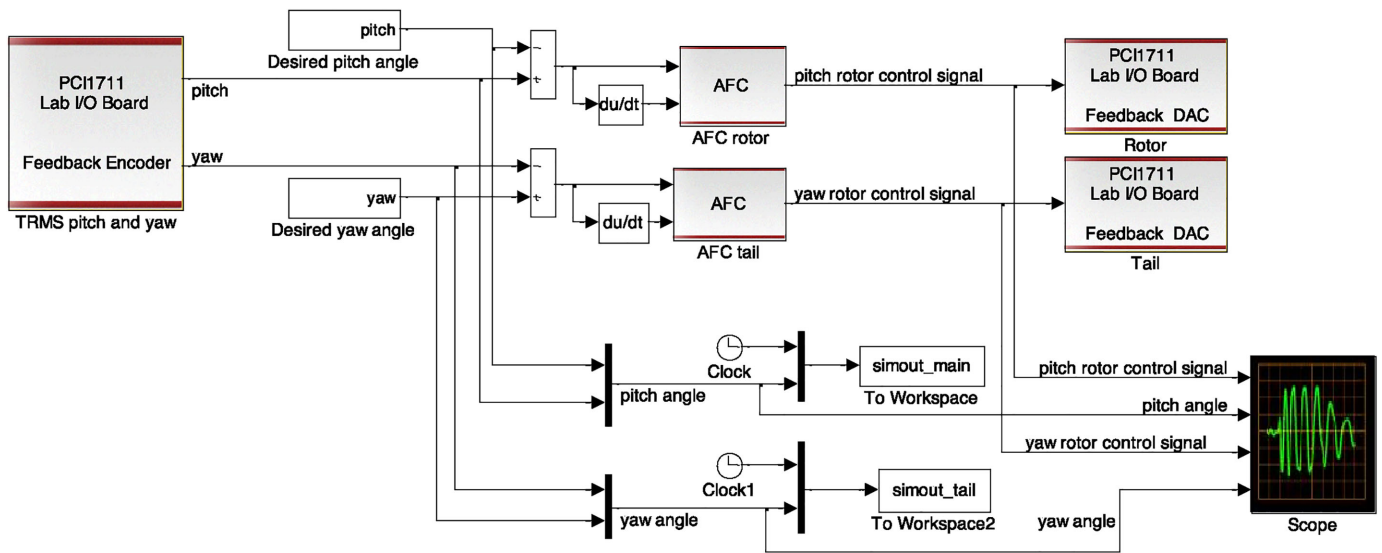
This article has been accepted for inclusion in a future issue of this journal. Content is final as presented, with the exception of pagination.

8                                                                                                          IEEE SYSTEMS JOURNAL



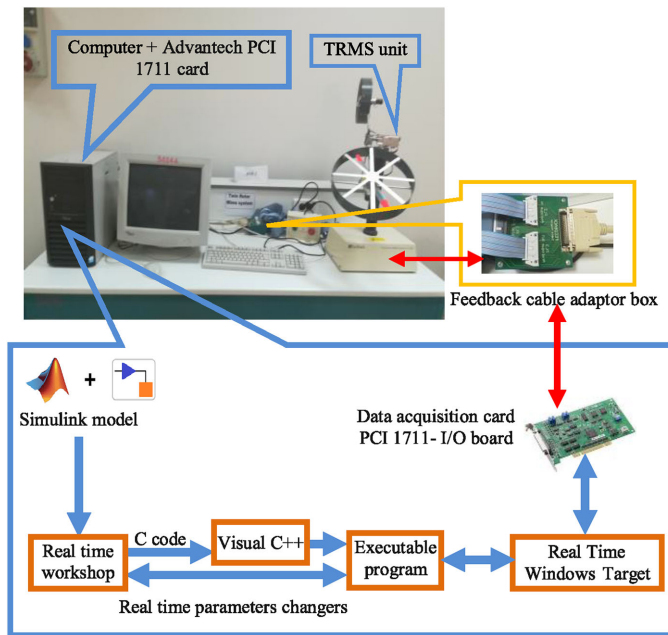Fig. 4.    Complete MATLAB/Simulink block of wind disturbance rejection.
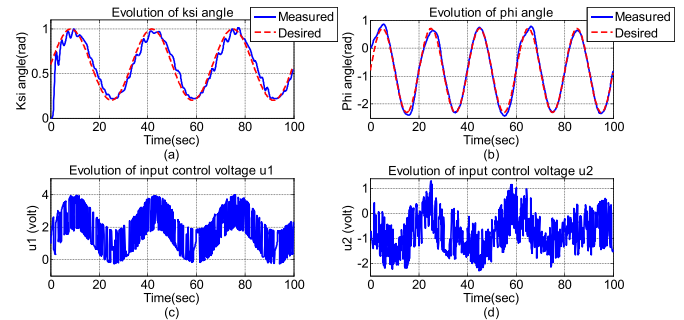


Fig. 5.    Experimental workbench of the TRMS.



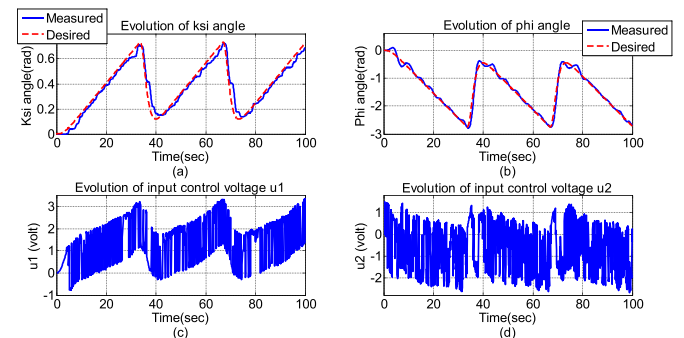Fig. 6.    Experimental results for sine wave tracking.



Fig. 7.    Experimental results for sine wave tracking with different frequencies.



Fig. 8.    Experimental results for triangle wave tracking.
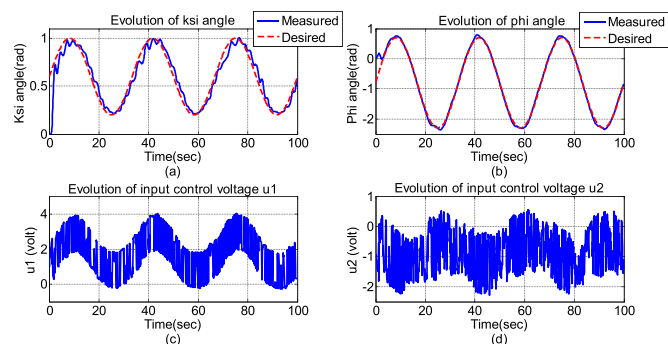
modification of desired signals by preserving the regulated positions as shown in Fig. 10(a) and (b). The tracking responses of square desired trajectory with different frequencies is performed with experimentation as presented in Fig. 11(a) and (b). These figures prove the capability of the developed control method to deal with different coupling of the two subsystems, after small transient perturbations in the experimental responses of pitch and yaw angles as shown in Fig. 10(a) and (b) due to

This article has been accepted for inclusion in a future issue of this journal. Content is final as presented, with the exception of pagination.

ZEGHLACHE *et al.*: TWIN ROTOR MIMO SYSTEM EXPERIMENTAL VALIDATION OF ROBUST ADAPTIVE FUZZY CONTROL 9
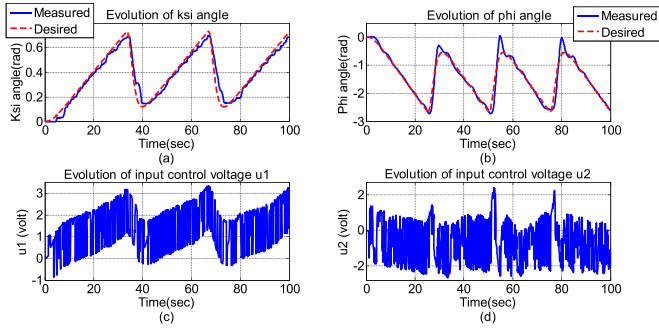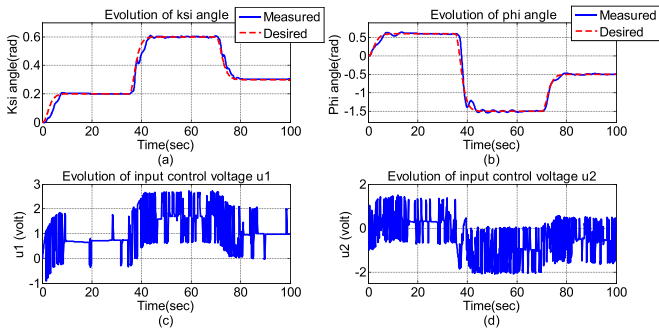


Fig. 9. Experimental results for triangle wave tracking with different frequencies.



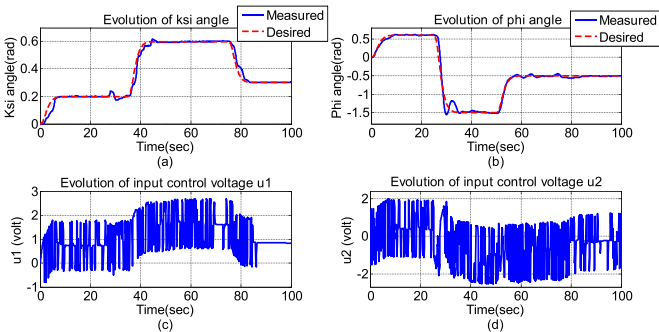Fig. 10. Experimental results for square wave tracking.



Fig. 11. Experimental results for square wave tracking with different frequencies.

the intermittent nature of the square signals. The control input signals presented in experimental results shown in Fig. 10(c) and (d) and Fig. 11(c) and (d) are limited to the permit interval.

### D. Test4: Experimental Tracking in Presence of Wind Effects

In order to confirm the robustness of the developed control algorithm, wind disturbances are introduced experimentally by a fan placed closer to TRMS. Thus, the average wind speed rise up to around 3.8 m/s, as shown in Fig. 12. It is practically verified that the TRMS can withstand maximum speed of around 5 m/s. The obtained results are presented in Figs. 13–15.

Fig. 13(a) and (b), Fig. 14(a) and (b) and Fig. 15(a) and (b), show the absolute position of the TRMS in vertical and
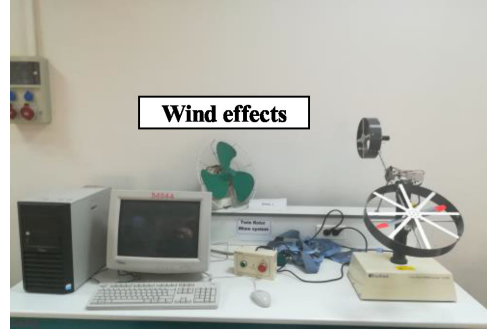


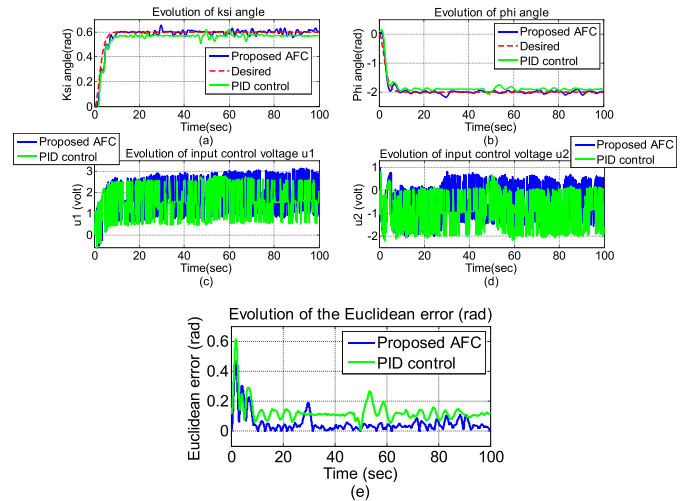Fig. 12. Experimental workbench of the TRMS in presence wind effects.



Fig. 13. Experimental results for step wave tracking in presence of wind effects.

horizontal plan, when the wind force are introduced. The tracking tasks are successfully effectuated and the desired trajectories are tracked with high precision. Consequently, the developed control algorithm attains a good rejecting of the external disturbances which demonstrates a good robustness. It is also observed that in Figs. 13 and 14(c) and (d) and Fig 15 the control voltage signals are restricted in the permit interval and the consumed energy is minimized.

A comparison between the tracking problem in presence of wind effects obtained using the proposed controller and the PID control, have been performed experimentally on the TRMS. The tracking responses of two controllers are illustrated in Figs. 13 14 and 15(a) and (b). Therefore, as shown in these figures, the Euclidean error of the proposed controller is a significantly smaller than that of the conventional controller, due to the adaptive learning capabilities of the proposed AFC strategy.

For quantitative comparison between two previous control methods, root-mean-square error (RMSE) is used as a comparison criteria. Table III and Fig. 16 show the RMSE values of the experimental results in presence of external disturbances (wind effects) using the PID control and the proposed AFC approach. It is observed that the proposed AFC offers the smallest values control of RMSE, whereas the PID control presents the largest

This article has been accepted for inclusion in a future issue of this journal. Content is final as presented, with the exception of pagination.

10                                                                                                                    IEEE SYSTEMS JOURNAL
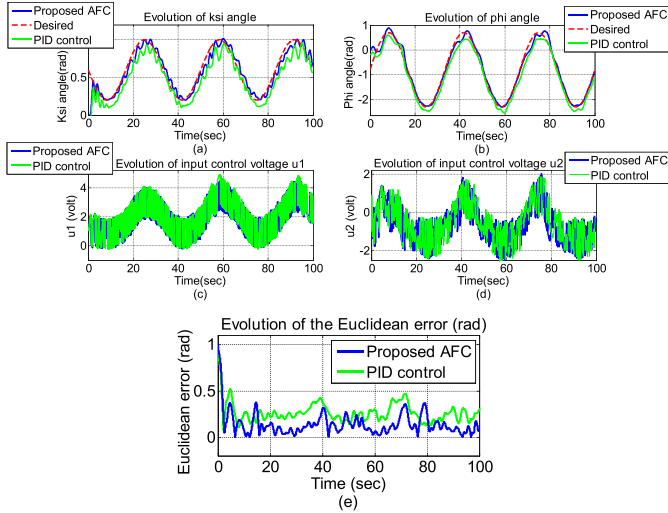
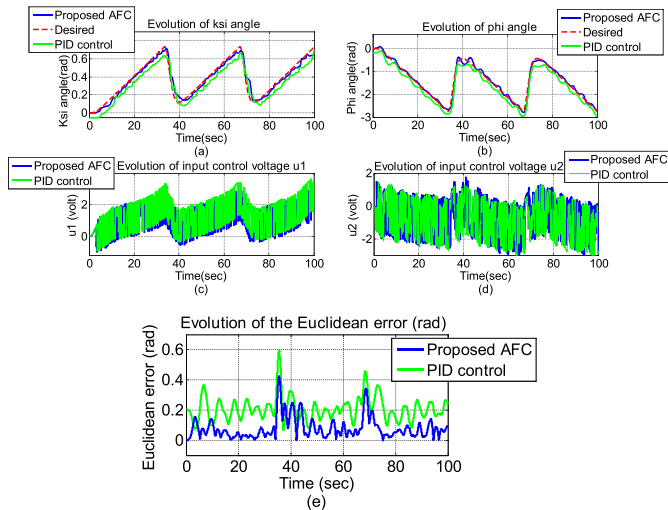Fig. 14.    Experimental results for sin wave tracking in presence of wind effects.



Fig. 15.    Experimental results for triangle wave tracking in presence of wind effects.

TABLE III
RMSE VALUES FOR THE PROPOSED AFC AND PID CONTROL

| Scenario | Controller Types | RMSE values (rad) |
|---|---|---|
| Step wave tracking | Proposed AFC | 0.0823 |
| | PID control | 0.143 |
| Sine wave tracking | Proposed AFC | 0.187 |
| | PID control | 0.281 |
| Triangle wave tracking | Proposed AFC | 0.105 |
| | PID control | 0.222 |

values of RMSE. It can be seen that the system performances are better, when using the proposed AFC as compared to the PID control controller.

### E.  Test5: Robustness evaluation

To evaluate the robustness of the TRMS with the developed controller, another type of external disturbance is added by
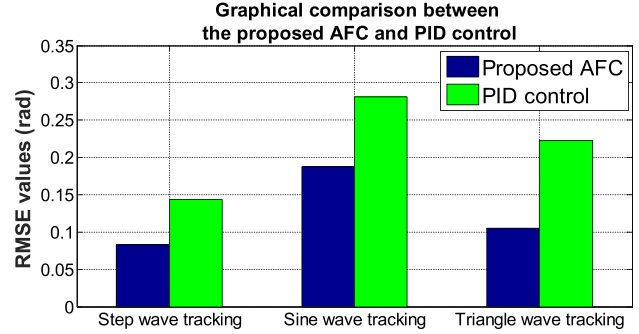


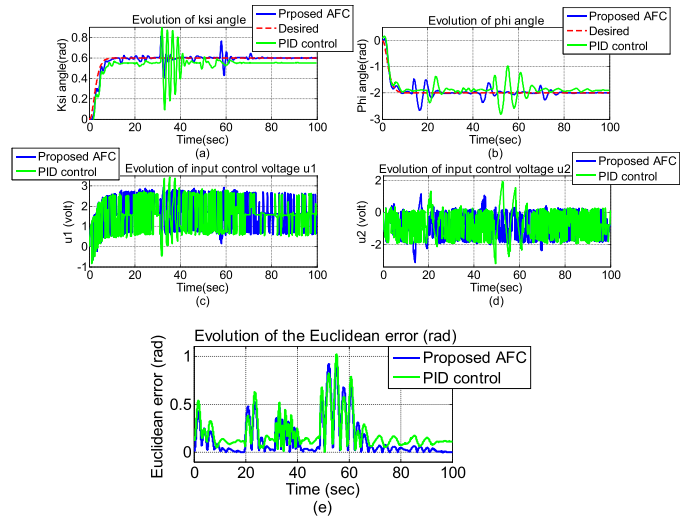Fig. 16.    RMSE Histogram of the proposed AFC and PID control.



Fig. 17.    Step responses of the TRMS subject to the external disturbance.

giving a small jerk to the vertical and horizontal rotors. From the experimental results of the TRMS presented in Fig. 17(a) and (b), it is noticed that the TRMS with the developed controller is robust to external disturbances. As shown in Fig. 17(c) and (d) a peaking phenomena occurs in the input control signals to overcome the abrupt variations of TRMS angles provoked by external disturbances. From experimental results, the developed control algorithm proves a good capability of trajectory tracking and admissible calculation time.

The Euclidean error values for different controllers are shown in Fig. 17(e). It can be seen that the proposed AFC yields a superior performance than that of the conventional PID controller.

### V.  CONCLUSION

In this article, an AFC has been developed to control the TRMS in real time. The system stability in the closed-loop has been demonstrated by Lyapunov method, in which all adaptive laws have been generated in order to augment the robustness versus wind gusts, external disturbances and uncertainties. The performance of the proposed controllers has been tested with different desired signals and it has been shown that the TRMS can follow the reference trajectories with good performances.

The experimental results prove the good tracking performance of the proposed control strategy in the presence of uncertainties, wind gusts and external disturbances. Eventually, as future work, a global fast dynamic terminal sliding mode control based on adaptive radial basis function neural network will be addressed to the TRMS in order to improve the tracking performances. Videos of experiments are available online.[1,2]

## REFERENCES

[1] M. Mones and T. Diaa-Eldeen, "Experimental nonlinear identification of a lab-scale helicopter system using MLP neural network," in *Proc. 13th Int. Comput. Eng. Conf.*, 2017, pp. 166–171.

[2] M. Ahmad, A. Ali, and M. A. Choudhry, "Fixed-structure H∞ controller design for two-rotor fixed-structure," *Arab J Sci Eng.*, vol. 41, no. 9, pp. 3619–3630, 2016.

[3] D. M. Ezekiel, R. Samikannu, and O. Matsebe, "Pitch and yaw angular motions (rotations) control of the 1-DOF and 2-DOF TRMS: A survey," *Arch. Comput. Methods Eng.*, to be published, doi: 10.1007/s11831-020-09423-3.

[4] S. J. Petkar, A. A. Gupta, V. B. Ketkar, and F. S. Kazi, "Robust model predtictive control of PVTOL aircraft," in *Proc. IFAC-PapersOnLine*, 2016, pp. 760–765.

[5] P. Wen and T. W. Lu, "Decoupling control of a twin rotor MIMO system using robust deadbeat control technique," *IET Control Theory Appl.*, vol. 2, no. 11, pp. 999–1007, 2008.

[6] J. G. Juang, M. T. Huang, and W. K. Liu, "PID control using presearched genetic algorithms for a MIMO system," *IEEE Trans. Syst., Man, Cybern.:PartC*, vol. 38, no. 5, pp. 716–727, Sep. 2008.

[7] V. K. Pandey, I. Kar, and C. Mahanta, "Control of twin rotor MIMO system using multiple models with second level adaptation," *IFAC-Papers Line*, vol. 49, no. 1, pp. 676–681, 2016.

[8] S. Singh, S. Janardhanan, and U. N. Mashoq, "Fast terminal sliding mode control for TRMS," in *Proc. Annu. IEEE India Conf.*, 2015, pp. 1–5.

[9] S. Zeglache, K. Kara, and D. Saigaa, "Type-2 fuzzy logic control of a 2-DOF helicopter," *Central Eur. J. Eng.*, vol. 4, no. 3, pp. 303–315, 2014.

[10] T. S. Mahmoud, M. H. Marhaban, T. S. Hong, and N. Sokchoo, "ANFIS controller with fuzzy subtractive clustering method to reduce coupling effects in twin rotor MIMO system (TRMS) with less memory and time usage," in *Proc. Int. Conf. Adv. Comput. Control*, 2009, pp. 19–23.

[11] C. W. Tao, S. Taurb, and Y. C. Chen, "Design of a parallel distributed fuzzy LQR controller for the twin rotor multi-input multi-output system," *Fuzzy Sets Syst.*, vol. 161, no. 15, pp. 2081–2103, 2010.

[12] A. Rahideh and M. H. Shaheed, "Real time hybrid fuzzy-PID control of a twin rotor system," in *Proc. Int. Conf. Mechatronics*, 2009, pp. 1–6.

[13] B. Pratap and S. Purwar, "Real-time implementation of neuro adaptive observer-based robust backstepping controller for twin rotor control system," *J Control Autom Electr Syst*, vol. 25, no. 2, pp. 137–150, 2014.

[14] S. Mondal and C. Mahanta, "Adaptive second-order sliding mode controller for a twin rotor multi-input multi-output system," *IET Control Theory*, vol. 14, no. 6, pp. 2157–2167, 2012.

[15] M. Chemachema and S. Zeghlache, "Output feedback linearization based controller for a helicopter-like twin rotor MIMO system," *J. Intell. Robot System*, vol. 48, no. 1, pp. 181–190, 2008.

[16] J. G. Juang, M. T. Huang, and W. K. Liu, "PID control using presearched genetic algorithms for a MIMO system," *IEEE Trans. Syst. Man Cybern.: Part C.*, vol. 38, no. 5, pp. 716–727, Sep. 2008.

[17] J. G. Juang,, W. K. Liu, and R. W. Lin, "A hybrid intelligent controller for a twin rotor MIMO system and its hardware implementation," *ISA Trans*, vol. 50, no. 4, pp. 609–619, 2011.

[18] P. Wen and T. W. Lu, "Decoupling control of a twin rotor MIMO system using robust deadbeat control technique," *IET Control Theory Appl.*, vol. 38, no. 5, pp. 716–727, 2008.

[19] A. Rahideh, A. H. Bajodah, and M. H. Shaheed, "Real time adaptive nonlinear model inversion control of a twin rotor MIMO system using neural networks," *Eng. Appl. Artif. Intell.*, vol. 25, no. 6, pp. 1289–1297, 2012.

[20] J. G. Juang, R. W. Lin, and W. K. Liu, "Comparison of classical control and intelligent control for a MIMO system," *Appl. Math. Comput.*, vol. 15, no. 2, pp. 778–791, 2008.

[21] B. Loutfi, Z. Samir, D. Ali, and G. M. Zinelaabidine, "Real time implementation of type-2 fuzzy backstepping sliding mode controller for twin rotor MIMO system (TRMS)," *Traitement Du Signal*, vol. 36, no. 1, pp. 1–11, 2019.

[22] Y. J. Huang, H. W. Wu, and T. C. Kuo, "PID-based fuzzy sliding mode control for twin rotor multi-input multi-output systems," in *Proc. IEEE Tencon - Spring*, 2013, pp. 204–207.

[23] C. W. Tao, J. S. Taur, Y. H. Chang, and C. W. Chang, "A novel fuzzy sliding and fuzzy integral sliding controller design for the twin rotor multi-input multi-output system," *IEEE Trans. Fuzzy Syst.*, vol. 18, no. 2, pp. 1–12, Oct. 2010.

[24] R. Raghavan and S. Thomas, "Practically implementable model predictive controller for a twin rotor multi-input multi-output system," *J Control Autom Electr Syst*, vol. 28, no. 4, pp. 358–370, 2017.

[25] N. V. Chi, "Adaptive feedback linearization control for twin rotor multiple-input multiple-output system," *Int. J. Control Autom. Syst.*, vol. 15, no. 3, pp. 1267–1274, 2017.

[26] F. A. Shaik and S. Purwar, "A nonlinear state observer design for 2-DOF twin rotor system using neural networks," in *Proc. Int. Conf. Adv. Comput., Control, Telecommun. Technol.*, 2009, pp. 15–19.

[27] Twin Rotor MIMO System Manual. Feedback Instruments Ltd., UK, 2006. [Online]. Available: http://www.cpdee.ufmg.br/~palhares/33-942rotor.pdf

[28] S. Tong, Y. Li, G. Feng, and T. Li, "Observer-based adaptive fuzzy backstepping dynamic surface control for a class of MIMO nonlinear systems," *IEEE Trans. Syst., Man, Cybern., Part B Cybern.*, vol. 41, no. 4, pp. 1124–1135, Aug. 2011.

[29] L. X. Wang, *Adaptive Fuzzy Systems and Control: Design and Stability Analysis*. NJ, USA: Prentice-Hall, Inc, 1994.

[30] Y. Fouad, B. Omar, H. Mustapha, and R. Nassim, "Observer-based adaptive fuzzy backstepping tracking control of quadrotor unmanned aerial vehicle powered by li-ion battery," *J Intell Robot Syst*, vol. 84, no. 3, pp. 179–197, 2016.

[31] N. Bounar, A. Boulkroune, F. Boudjema, M. M'Saad, and M. Farza, "Adaptive fuzzy vector control for a doubly-fed induction motor," *Neurocomputing*, vol. 151, no. 2, pp. 756–769, 2015.

[32] A. Boulkroune, M. Tadjine, M. M'Saad, and M. Farza, "How to design a fuzzy adaptive controller based on observers for uncertain affine nonlinear systems," *Fuzzy Sets Syst.*, vol. 159, no. 8, pp. 926–948, 2015.

[33] A. Boulkroune, L. Merazka, and H. Li, "Fuzzy adaptive state-feedback control scheme of uncertain nonlinear multivariable systems," *IEEE Trans. Fuzzy Syst.*, vol. 27, no. 9, pp. 1703–1713, Sep. 2019.

[34] F. Wang, B. Chen, X. Liu, and C. Lin, "Finite-time adaptive fuzzy tracking control design for nonlinear systems," *IEEE Trans. Fuzzy Syst.*, vol. 26, no. 3, pp. 1207–1216, Jun. 2018.

[35] H. K. Tran, J. Chiou, N. T. Nam, and V. Tuyen, "Adaptive fuzzy control method for a single tilt tricopter," *IEEE Access*, vol. 7, pp. 161741–161747, 2019.

---

[1] https://youtu.be/XZCNQY3SDfI
[2] https://youtu.be/om4e64uLe9M